UNIVERSITY OF CALIFORNIA SAN DIEGO

The Antiviral Evolutionary Arms Race between IFITs and RNA Viruses

A Thesis submitted in partial satisfaction of the requirements for the degree Master of Science

in

Biology

by

Elena Danielle Estrada

Committee in charge:

Professor Matthew Daugherty, Chair
Professor Amy Pasquinelli, Co-Chair
Professor Kevin Corbett

2019

The Thesis of Elena Danielle Estrada is approved, and it is acceptable in quality and form for publication on microfilm and electronically:

Co-Chair

Chair

University of California San Diego

2019

TABLE OF CONTENTS

LIST OF FIGURES

ACKNOWLEDGEMENTS

I would like to acknowledge Professor Matthew Daugherty for his guidance and support throughout my academic career. I would also like to acknowledge the members of the Daugherty Lab whose patience and advice helped me succeed. In particular, the work of Dr. Agustina D'Urso and Candace Todd has greatly contributed to my project's success.

ABSTRACT OF THE THESIS

The Antiviral Evolutionary Arms Race between IFITs and RNA Viruses

by

Elena Danielle Estrada

Master of Science in Biology

University of California San Diego, 2019

Professor Matthew Daugherty, Chair
Professor Amy Pasquinelli, Co-Chair

The mammalian innate immune system serves as a first line of defense against pathogens. Innate immunity molecules are critical for initial recognition and inhibition of non-self targets. However, viruses rapidly evolve to evade these innate defenses. Therefore, to successfully mitigate pathogenesis, host proteins must adapt against evolving viruses. The effects of this antagonistic coevolution are evident in the genetic footprints of many innate immunity proteins such as interferon-induced with tetratricopeptide repeats (IFIT) proteins 2 and 3. Despite the ancestral gene duplication that gave rise to IFIT2 and IFIT3, there is one

region of high similarity between these two genes. Interestingly, this genetic similarity is due to recurrent recombination between IFIT2 and IFIT3. This co-evolutionary signature suggests that IFIT2 and IFIT3 may interact and share a common antiviral function. To understand how potential IFIT2/3 heterodimers inhibit infection, the antiviral activity of IFIT2 and IFIT3 were analyzed in Semliki forest virus (SFV), Thogoto virus (THOV), influenza A virus (IAV), and Ebola virus (EBOV) reporter assays. Our findings indicate that IFIT2/3 antiviral activity is mediated by two components: RNA binding and heterodimerization. We propose that key acidic and basic residues (IFIT2 E156, IFIT2 K158, IFIT3 E153, IFIT3 K156) in subdomain 2 of IFIT2 and IFIT3 are critical for viral RNA recognition. Consistent with our hypothesis that the recombining region may mediate heterodimerization, we find that IFIT2/3 interaction is disrupted by a single change (S111A) in the recombination region of subdomain 1 in IFIT2. Further analysis of the unique antiviral mechanism of IFIT2/3 will help predict which pathogens IFIT2/3 inhibit and provide insight into the host innate immune response.

INTRODUCTION

1.1 Innate Immunity

The mammalian innate immune system serves as a first line of defense against foreign invaders. Innate immunity molecules are critical for the initial recognition and inhibition of pathogens prior to the activation of more specific antiviral mechanisms (Uthaisangsook et al., 2002). Innate broad spectrum antiviral activity relies on sensors that identify non-self markers such as pathogen-associated molecular patterns (Mogensen, 2009) including foreign RNA (Schaefer et al., 2017). Pathogen-associated molecular patterns are evolutionarily conserved structures that are essential to pathogen survival, making them susceptible to non-self detection by innate immunity molecules (Mogensen, 2009). In addition, innate immunity proteins inhibit the production of viral proteins by targeting viral RNA. For example, mammalian host proteins can cleave viral RNA transcripts (Choi et al., 2015) or prevent viral RNA translation (García et al., 2006).

1.2 Mammalian Host Detection of Foreign RNA

In order to inhibit viral infection, mammalian innate immune sensors must first identify foreign RNA via features such as double-stranded RNA (dsRNA) (Reikine et al., 2014) and virus-specific capping structures (Fensterl & Sen, 2015; Loo & Gale, 2011) (Fig. 1). For instance, MDA5 is an innate immune receptor that associates with long viral double-stranded RNA regardless of RNA sequence or structure (Reikine et al., 2014). Another innate sensor, RIG-I, is an intracellular pattern recognition receptor that detects the 5'-triphosphate caps of viral dsRNA (Loo & Gale, 2011). Binding to foreign RNA often initiates downstream signaling, inducing the expression of cellular antiviral proteins such as interferons (IFNs).

IFNs activate the expression of hundreds of IFN-stimulated genes (ISGs) which act as the effectors of the innate immune system (Fleith et al., 2018) (Fig. 1).

ISGs combat a broad range of infections by targeting viral RNA and inhibiting viral protein production (Daugherty et al., 2016; Fensterl & Sen, 2015; Vladimer et al., 2014). Some effector molecules, such as oligoadenylate synthase-like (OASL) protein, degrade viral RNA. When bound to dsRNA, OASL oligomerizes, activating RNase L, an endoribonuclease that cleaves viral transcripts (Choi et al., 2015). Effectors also mitigate infection by inhibiting foreign RNA translation. Protein kinase R (PKR) is an ISG that self-activates when associated with foreign dsRNA. Auto-activated PKR inhibits the initiation of viral RNA translation by phosphorylating eukaryotic initiation factor 2. This phosphorylation enhances the translation of host mRNAs involved in stress response while inhibiting continued translation of other cellular and viral RNAs (García et al., 2006).

1.3 The Host-Virus Arms Race

The sensor and effector molecules of the innate immune system combat infection by recognizing viral characteristics such as specific dsRNA lengths and cap modifications. However, even with these defense strategies, hosts remain susceptible to viral infection. This is because viruses rapidly evolve to circumvent the antiviral mechanisms of innate immunity molecules (Daugherty & Malik, 2012). Just as viruses adapt to evade immune defenses, host sensors and effectors evolve to combat new viral infection strategies. This cyclical, antagonistic relationship is known as the host-virus arms race (Daugherty & Malik, 2012).

The constant evolutionary pressure for viruses to infect their targets and hosts to inhibit viruses has genetically altered host innate immunity proteins. For example, the genetic effects of antagonistic coevolution are evident in numerous ISGs such as interferon-induced

with tetratricopeptide repeats (IFIT) proteins (Daugherty et al., 2016). These highly-upregulated, rapidly evolving ISGs are known to mitigate pathogenesis via a variety of mechanisms, including inhibition of viral mRNA translation (Vladimer et al., 2014).

1.4 IFITs: Inhibiting Viral mRNA Translation

The number and identity of IFIT genes differs greatly between species, but most mammals carry IFIT1, IFIT1B, IFIT2, IFIT3, and IFIT5 (Daugherty et al., 2016). These structurally similar IFIT proteins are composed of helix-turn-helix tetratricopeptide repeats (TPRs)—34 amino acid sequences known to mediate protein-protein (Abbas et al., 2013) and protein-RNA (Diamond, 2014) interactions.

For example, mouse IFIT1B (MIFIT1B, formally known as mouse IFIT1) recognizes viral RNA that is unmethylated on the ribose sugar of the first transcribed nucleotide (cap0 structure) (Daffis et al., 2010; Daugherty et al., 2016). While many viral mRNAs have cap0 structures, mammalian host RNA is methylated at the first transcribed nucleotide (cap1 structure) (Diamond, 2014). MIFIT1B binds to the 5' end of cap0 mRNAs and inhibits viral translation by blocking binding of eIF4e, a eukaryotic translation initiation factor, to the viral mRNA. MIFIT1B has not been shown to inhibit "cap-snatching" viruses like influenza A which circumvent MIFIT1B recognition by deriving their 5' ends from host cell pre-mRNAs (Burgui et al., 2007).

In contrast, IFIT1 proteins, including human IFIT1 (HIFIT1) are able to restrict viruses that produce cap1-mRNAs (Daugherty et al., 2016). The positively-charged cavity of HIFIT1 interacts with the 5' end of viral mRNA, inhibiting translation (Fensterl & Sen, 2015). For instance, HIFIT1 displays antiviral activity in Semliki forest virus (SFV) reporter assays and Sindbis viral infections (Candace Todd, unpublished data). These viruses are related to

prevalent *Alphaviruses* like Chikungunya virus which is spread to humans via mosquitos (Centers for Disease Control and Prevention, 2018).

Although the antiviral activity of MIFIT1B and HIFIT1 is relatively well understood, the exact molecular mechanisms that allow IFIT2 and IFIT3 to distinguish non-self RNA remain unclear. However, like MIFIT1B and HIFIT1, IFIT2 and IFIT3 may rapidly evolve against viruses. This suggests that genetic analysis of IFIT2 and IFIT3 will help determine the effects of virus-mediated coevolution and help identify IFIT2- and IFIT3-specific viral RNA targets.

1.5 IFIT2/3: Proposed Coevolution and Oligomerization

Despite shared sequence homology between IFIT2 and IFIT3 (amino acid residues ~67 to ~121), evolutionary analyses reveal that IFIT2 and IFIT3 have consistently mutated over time. For conservation in this region to occur despite these mutations, IFIT2 and IFIT3 must frequently exchange their genetic material through recombination (Daugherty, unpublished data). This recurrent recombination allows IFIT2 and IFIT3 to remain homologous even when one of the proteins evolves. However, recombination such as this is extremely rare, suggesting that there is a selective pressure that drives IFIT2 and IFIT3 to coevolve. In the case of two host defense proteins such as IFIT2 and IFIT3, a non-deleterious mutation in one that would be compatible with a random mutation in the other is unlikely to occur numerous times (Daugherty & Malik, 2012). Therefore, in order for IFIT2 and IFIT3 to coevolve, a pathogen likely acts as an antagonist to their antiviral function. This pathogen-mediated coevolution may involve oligomerization such that a pathogen may physically interact with both proteins at once.

Indeed, IFIT research has highlighted the propensity of IFITs to interact with each other (Fleith et al., 2018; Pichlmair et al., 2011). Preliminary research into such oligomerization reveals that IFITs form a multiprotein complex. IFIT1, IFIT2, and IFIT3 co-immunoprecipitate together out of interferon-induced cells, indicating that there is an interaction between the three proteins (Pichlmair et al., 2011). Further research has demonstrated that IFIT2 self-associates, forming a homodimer by swapping two and a half N-terminal TPRs (Yang et al., 2012). The amino acids necessary for IFIT2 dimerization are conserved between IFIT2 and IFIT3 (Mears & Sweeney, 2018), suggesting that IFIT3 may homodimerize similarly to IFIT2. This 70% homologous N-terminal sequence between IFIT2 and IFIT3 also suggests that IFIT2 and IFIT3 can form a heterodimer that is structurally similar to the IFIT2 homodimer. Indeed, a recent study demonstrates that IFIT2 and IFIT3 heterodimerize and that the IFIT2/3 heterodimer is more stable than either homodimer (Fleith et al., 2018). Thus, the dimer interface of IFIT2 may allow for heterodimerization. This characteristic supports coevolution analyses and encourages further analyses of potential IFIT2/3 heterodimerization and cofunction.

1.6 IFIT2/3 Heterodimer: Salt Bridge Model

Initial research into the structural nature of such heterodimers stems from the predicted IFIT2 structure which contains an extensive nucleotide-binding channel rich with positively charged residues (Yang et al., 2012). Taking both potential RNA interaction and the IFIT2 crystal structure into account, we developed a preliminary model for IFIT2/3 heterodimerization (Fig. 6C) in which IFIT2 and IFIT3 bind RNA in a similar location and fashion. In this model, acidic and basic amino acids face away from the proposed RNA binding site, on the other side of the RNA-mediating alpha helix (Daugherty, unpublished

data). These residues are conserved in human IFIT2 (HIFIT2), human IFIT3 (HIFIT3), mouse IFIT2 (MIFIT2), and mouse IFIT3 (MIFIT3). We proposed that salt bridges may link these charged groups in a swapped dimer fashion such that IFIT2 acidic residues interact with IFIT3 basic residues and vice versa (Fig. 6C).

Functional assays were utilized to characterize the biochemical and molecular consequences of these potential salt bridges. Point mutations in IFIT2 and IFIT3 were created to disrupt two putative salt bridges. The antiviral activity of wild type (WT) and mutant IFIT2/3 heterodimers was analyzed in viral reporter systems (Semliki forest virus (SFV), Thogoto virus (THOV), and influenza A virus (IVA), Ebola virus (EBOV)). When mutated, the antiviral functionality of the heterodimer was inhibited (Fig. 7). This demonstrates that the antiviral activity of IFIT2/3 is mediated by several key charged residues in subdomain 2 of IFIT2 and IFIT3.

However, when considered in the context of the HIFIT1 crystal structure (Abbas et al., 2017), the proposed IFIT2/3 salt bridge model may not enable both dimerization and RNA binding. The structure of the RNA binding pocket in HIFIT1 (Fig. 2B) is quite compact, with folds close to the acidic and basic residues discussed above. Therefore, in order for IFIT2/3 heterodimerization to occur, RNA may not bind to IFIT2 and IFIT3 the same way that it binds to HIFIT1. An alternative hypothesis is that these charged residues may confer RNA interaction, but not heterodimerization. Indeed, co-immunoprecipitation results revealed that these same charge-swap mutations heterodimerize as well as WT IFIT2 and IFIT3 (Agustina D'Urso, unpublished data), despite a complete loss of antiviral activity in viral reporter systems.

1.7 IFIT2/3 Heterodimer: Recombination Model

Hence, another IFIT2/3 heterodimer model was created. Recurrent recombination between IFIT2 and IFIT3 suggests that the two proteins coevolve with each other, possibly as a way to antagonistically evolve against a pathogen (Daugherty & Malik, 2012). This frequent exchange of genetic material suggests that IFIT2 and IFIT3 may function as a heterodimer. If this is the case, the recombination region of IFIT2 and IFIT3 may also serve as the dimerization site. This is because the genetic exchange point likely occurs in a location where IFIT2 and IFIT3 are in close proximity, or interacting.

In this second heterodimer model (Fig. 8), IFIT2 and IFIT3 are inverted such that the recombination regions are facing each other. Similarly to the salt bridge model, point mutations (MIFIT2 Q72A, MIFIT2 G75K, MIFIT2 S111A, MIFIT2 S111A-D118A, MIFIT3 D79T, MIFIT3 S83A, MIFIT3 S111A, MIFIT3 A115T, MIFIT3 Q122K) were created on both IFIT2 and IFIT3 to test functionality and interaction. Amino acid residues were mutated if they were conserved between IFIT2 and IFIT3, but not in MIFIT1B or HIFIT1. This is because differential conservation helps identify specific residues as critical for IFIT2/3-mediated antiviral activity, but not necessarily MIFIT1B or HIFIT1-mediated antiviral activity.

SFV reporter assays were utilized to characterize the biochemical and molecular consequences of these specific amino acids. The antiviral functionality of the heterodimer was inhibited (Fig. 9) when key amino acid S111 in the recombination region of MIFIT2 was mutated. This demonstrates that the antiviral activity of MIFIT2/3 is mediated by the key components of the recombination region in subdomain 1 of MIFIT2.

1.8 IFIT2/3 Heterodimerization and Antiviral Activity

Virus-mediated antagonism of IFIT2 and IFIT3 promotes IFIT2/3 coevolution. Sequence homology between these two coevolving proteins indicates that IFIT2 and IFIT3 function as a heterodimer. The propensity of IFIT2 and IFIT3 to oligomerize suggests that their binding specificity and antiviral mechanism is distinct from that of MIFIT1B and HIFIT1 which often work as individual effectors against viral mRNA. Analyzing the antiviral activity of mutated IFIT2/3 heterodimers will elucidate how IFIT proteins prevent viral replication, help to predict which pathogens may be inhibited by IFIT2/3 dimers, and provide insights into the mechanisms of host innate immune response.

MATERIALS AND METHODS

2.1 Cloning in pAR097

WT and mutant IFITs were cloned into a parental plasmid (pAR097) that allows for the co-expression of two genes separated by a P2A site (Fig. 3). P2A results in a ribosome stalling, terminating, and reinitiating translation. This allows the same ribosome to translate two distinct proteins at comparable levels (Fan, 2014).

The P2A site enables pAR097 to serve as a multicistronic vector that can be utilized for various applications. For example, transfection efficiency can be analyzed by inserting mCherry and a gene of interest into pAR097. The P2A site also allows for co-expression of IFIT2 and IFIT3, which is beneficial for simultaneous expression of both proteins. In addition, due to limitations in transfection scale and efficiency, transfection with a single plasmid containing both IFIT2 and IFIT3 ultimately leads to higher concentrations of IFIT2 and IFIT3 (i.e. 400 ng each) when compared to co-transfection of individual IFIT2 and IFIT3 plasmids (i.e. 200 ng each). pAR097 was used for all transfections for Semliki forest virus reporter assays, Thogoto virus minireplicon assays, influenza minigenome reporter assay, Ebola virus minigenome reporter assay, and co-immunoprecipitations.

In addition, Flp-In™ 293 T-REx cell lines are compatible with pAR097, a Flp-In™ expression vector. Co-transfection of pAR097 with the Flp recombinase vector pOG44 targets pAR097 integration to the FRT site, a transcriptionally active locus in every Flp-In™ 293 T-REx cell (Invitrogen, 2010). pAR097 also contains a Dox-inducible promoter such that dox controls pAR097 gene expression. In summary, pAR097 allows for Dox-induced expression of WT and mutant IFIT2/3 at a stable locus, ensuring homologous gene expression levels.

These stable cell lines may then be infected with live virus such that the antiviral effects of WT and mutant IFIT2/3 may be observed.

2.2 Semliki Forest Virus Reporter Assay

Semliki forest virus (SFV) Reporter Assay utilizes the pSMART (*S*FV, *M*ammalian RNA-polymerase II dependent promotor, *A*ffinity tags, *R*estriction site expansion, *T*ranslation enhancer) vector to produce recombinant SFV with a beta-galactosidase reporter (Fig. 4B). Transfection of mammalian cells with pSMART leads to the production of SFV non-structural proteins which replicate DNA and amplify the mRNA encoding SFV structural proteins (DiCiommo et al., 2004). This results in increased expression of pSFV3-CMV-lacZ-pA, which turns on the beta-galactosidase reporter gene. When 4-methylumbelliferyl-β-D-galactopyranoside (4-MUG) is cleaved by beta-galactosidase, it generates the fluorophore 4-methylumbelliferone whose fluorescence can be monitored by a fluorescent plate reader (G-Biosciences, 2019). Low levels of beta-galactosidase reporter output as measured by fluorescence indicate antiviral activity. This occurs when co-transfected antiviral proteins inhibit expression of pSFV3-CMV-lacZ-pA, thereby reducing beta-galactosidase expression.

The SFV Reporter Assay was performed in 293T cells in a 24-well format. Two negative controls of 500 ng of empty pAR097 and four positive controls of 100 ng pSMART and 400 ng of empty pAR097 were transfected. 100 ng of pSMART and 400 ng of the gene(s) of interest in pAR097 were co-transfected in triplicate. Each transfection solution was incubated for 30 minutes with 1.5 µl of TransIT-X2® (Mirus Bio).

For complete cell lysis 24 hours post-transfection, the plate was frozen at -80ºC, thawed at 37ºC, frozen at -80ºC, thawed at 37ºC, frozen at -80ºC, and thawed at 37ºC. 5 mL of 37ºC optiMEM and 200 ul of 15 mg/ml 4-MUG in DMSO were mixed. 200 ul of this

solution was added to each well of lysed cells. The plate was rocked to mix thoroughly and analyzed using a BioTek Instruments, Inc. Cytation 5 plate reader. The imaging procedure was designed for a 24-well plate with a setpoint of 37ºC with a gradient of 0ºC. The machine read fluorescence endpoints in 20 second intervals for a 40 minute time period, equating to 121 reads per plate. The read speed was normal with a delay of 100 milliseconds and a height of 7 millimeters. The filter was set with an excitation of 365/20 and an emission of 445/20 with top optics, extended gain, xenon flash, high lamp energy, and extended dynamic range.

The average slopes (difference between reader outputs every 20 seconds) were calculated. The average slope over its standard deviation was determined for each time point. The maximum sum of these ratios was chosen as the time point of analysis. The average slopes at the maximum sum of ratios time point were averaged per condition to obtain an average fluorescence output per transfected gene(s) of interest. To account for variance, the average fluorescence output for the negative control was subtracted from the average fluorescence outputs of each condition. These data were then normalized by the positive control. The positive control had a viral reporter output of one. Values less than one were taken to be a percentage of viral reporter output, meaning that the protein(s) of interest displayed antiviral activity.

2.3 Thogoto Virus Minireplicon Assay

A minireplicon assay was used to analyze the antiviral activity of IFITs on thogoto virus (THOV) (Fig. 4C). Minireplicon systems utilize synthetic analogs of genomic RNA to analyze viral replication and host-virus interactions (Su et al., 2015). The THOV minireplicon system consists of four gene segments: three polymerase subunits (PA, PB1, and PB2) and the THOV nucleoprotein (NP), a key component of THOV replication machinery (Weber et al.,

2000). These components allow for the transcription of pHH21-vNP-FF-Luc, a viral transcript with a luciferase reporter gene. A control reporter, pTK-luc (Renilla) allows for normalization of luciferase luminescence based on cellular interference.

The THOV minireplicon assay was performed in 293T cells in a 24-well format and read on a 96-well plate. An empty control was made with 16 ng of PB2, PB1 and PA in pCAGGs vector, 4 ng of NP in pCAGGs vector, 80 ng of pHH21-vNP-FF-Luc (firefly luciferase), 50 ng pTK-Renilla (Promega), and 200 ng of empty pAR097. For each additional condition, 16 ng of PB2, PB1 and PA in pCAGGs vector, 4 ng of NP in pCAGGs vector, 80 ng of pHH21-vNP-FF-Luc (firefly luciferase), 50 ng pTK-Renilla (Promega) were co-transfected with 200 ng of various combinations of IFITs in pAR097. Each transfection solution was incubated for 30 minutes with 1.5 µl of TransIT-X2® (Mirus Bio). All conditions were done in triplicate.

24 hours post-transfection, the growth medium was removed and 100 ul of fresh media was added to each well. 75 µl of Dual-Glo® Luciferase Reagent was added to each well to lyse the transfected cells. After 10 minutes, the contents of the 24-well plate were added to a 96-well plate. The firefly luciferase activity (experimental expression) was then measured using a BioTek Instruments, Inc. Cytation 5 plate reader. The imaging procedure was designed for a 96-well plate with a setpoint of 22ºC with a gradient of 0ºC. The machine read luminescence endpoints with an integration time of 1 second. The read speed was normal with a delay of 100 milliseconds and a height of 1 millimeter. The filter had a full light emission, auto scale gain, top optics, and extended dynamic range. The Dual-Glo® Stop & Glo® substrate was diluted 1:100 in Dual-Glo® Stop & Glo® Buffer. 75 µl reagent was added to each well and incubated at room temperature for 10 minutes. The 96-well plate was then read

for Renilla luminescence (control expression) in the same order and under the same conditions as Firefly luminescence. Firefly expression (experimental reporter) was normalized to Renilla expression (control reporter) to distinguish IFIT-induced antiviral response and nonspecific cellular activities. For complete protocol details, refer to the Dual-Glo® Luciferase Assay System Technical Manual (Promega, 2015).

2.4 Influenza A Virus Minigenome Reporter Assay

The influenza A virus (IAV) minigenome system functions similarly to that of THOV and serves as a useful tool for exploring the viral activity of IAV (Fig. 4C). The minigenome plasmid contains a viral 5' and 3' end which flank a reporter gene and T7 polymerase. RNA polymerase I, and RNA polymerase II promotors and terminators. The viral UTRs on either end contain essential IAV regulatory elements while the reporter replaces the viral open reading frame, allowing for expression of an artificial gene (firefly luciferase) that can be quantified (Su et al., 2015). Like the THOV system, three polymerase subunits (PA, PB1, and PB2) and the IAV nucleoprotein (NP), a key component of IAV replication machinery (Weber et al., 2000) are necessary for viral expression. These components allow for the transcription of pPoll-Luc-H5N1, the viral transcript with the luciferase reporter gene. A control reporter, pTK-luc (Renilla) allows for normalization of luciferase luminescence based on cellular interference.

The IAV minireplicon assay was performed in 293T cells in a 24-well format and read on a 96-well plate. An empty control was made with 16 ng of PB2, PB1 and PA in pCAGGs vector, 4 ng of NP in pCAGGs vector, 80 ng of pPoll-Luc-H5N1 (firefly luciferase), 50 ng pTK-Renilla (Promega), and 200 ng of empty pAR097. For each additional condition, 16 ng of PB2, PB1 and PA in pCAGGs vector, 4 ng of NP in pCAGGS vector, 80 ng of pHH21-

vNP-FF-Luc (firefly luciferase), 50 ng pTK-Renilla (Promega) were co-transfected with 200 ng of various combinations of IFITs in pAR097. Each transfection solution was incubated for 30 minutes with 1.5 µl of TransIT-X2® (Mirus Bio). All conditions were done in triplicate. 24 hours post-transfection, the 24-well plate was analyzed for Firefly and Renilla luminescence as discussed in the THOV Minireplicon Assay protocol (see 2.3) the Dual-Glo® Luciferase Assay System Technical Manual (Promega, 2015).

2.5 Ebola Virus Minigenome Reporter Assay

The ebola virus (EBOV) minigenome consists of the 3' and 5' ends of the EBOV genome and a non-viral firefly luciferase reporter (Cressey, 2016) (Fig. 4C). Four viral proteins are necessary for transcription and replication: polymerase cofactor VP35, transcription activator VP30, a core component of RNA polymerase L, and nucleoprotein NP (Mühlberger, 2007). A control reporter, pTK-Renilla allows for normalization of luciferase luminescence based on cellular interference (Promega, 2015).

The EBOV minigenome reporter assay was performed in 293T cells in a 24-well format and read on a 96-well plate. An empty control was made with 37.5 ng of VP35 in pTM1 vector, 12.5 ng of VP30, 100 ng of L in pTM1 vector, 37.5 ng of NP in pTM1 vector, 25 ng of T7opt in pCAGGs vector, 25 ng 3E-5E-FF-Luc (firefly luciferase), 5 ng pTK-Renilla (Promega) and 242.5 ng of empty pAR097. For each additional condition37.5 ng of VP35 in pTM1 vector, 12.5 ng of VP30, 100 ng of L in pTM1 vector, 37.5 ng of NP in pTM1 vector, 25 ng of T7opt in pCAGGs vector, 25 ng 3E-5E-FF-Luc (firefly luciferase), 5 ng pTK-Renilla (Promega) were co-transfected with 242.5 ng of various combinations of IFITs in pAR097. Each transfection solution was incubated for 30 minutes with 1.5 µl of TransIT-X2® (Mirus Bio). All conditions were done in triplicate. 24 hours post-transfection, the 24-well plate was

analyzed for Firefly and Renilla luminescence as discussed in the THOV Minireplicon Assay protocol (see 2.3).

2.6 Statistical Analysis

All reporter assay conditions were done in triplicate, except in SFV reporter assays where four positive controls and two negative controls were transfected. Paired, two-tailed t-tests were performed in Excel to determine the statistical differences between various assay conditions.

RESULTS

3.1 IFIT2/3 Heterodimer

The antiviral activity of the WT IFIT2/3 heterodimer was analyzed in SFV reporter assays, THOV minireplicon assays, IAV minigenome reporter assays, and EBOV minireplicon assays.

SFV is a positive-stranded RNA *Alphavirus* that is able to infect its hosts with capped RNA (Ahola et al., 1999). The SFV reporter assay analyzes recombinant SFV expression with a beta-galactosidase reporter that can cleave 4-MUG, generating a fluorophore. When antiviral proteins inhibit recombinant SFV expression, beta-galactosidase production is inhibited, resulting in reduced fluorescence. When human and mouse WT IFIT2 and IFIT3 are co-transfected against the SFV reporter system, fluorescence is significantly reduced (Figs. 5A & 5B), indicating antiviral activity.

THOV is a negative-stranded ssRNA *Orthomyxovirus* with capped mRNAs (Weber et al., 1996). The THOV minireplicon assay utilizes a nucleoprotein and three polymerase subunits to transcribe a recombinant THOV transcript with a luciferase reporter gene. Inhibition of viral reporter expression by antiviral proteins results in reduced luminescence. In THOV assays, both human and mouse WT IFIT2/3 lead to reduced luminescence (Figs. 5C & 5D), indicating antiviral activity .

IAV is a negative-stranded ssRNA *Orthomyxovirus* with host-derived mRNA caps (Stevaert & Naesens, 2016). The IAV minigenome system functions similarly to the THOV assay with three polymerase subunits and the IAV nucleoprotein. These components transcribe a recombinant IAV transcript with the luciferase reporter gene. Reduced reporter expression by antiviral proteins results in reduced luminescence. In the IAV minigenome

system, MIFIT2/3 significantly reduces IAV viral output (Fig. 5E), indicating antiviral activity.

EBOV is a negative-sense ssRNA virus (Cressey, 2016). The EBOV minigenome works similarly to the THOV and IAV systems. Four EBOV non-structural proteins are necessary for transcription and replication of a firefly luciferase reporter which represents viral activity. In the EBOV minigenome system, MIFIT2/3 significantly reduces EBOV viral output as indicated by decreased firefly luminescence (Fig. 5F). This suggests that MIFIT2/3 is antiviral against EBOV.

3.2 IFIT2/3 Salt Bridge Mutation Model

In the salt bridge heterodimer model (Fig. 6), MIFIT2 E156 is predicted to interact with MIFIT3 K156 while MIFIT2 K158 is predicted to interact with MIFIT3 E153. Mutations to these acidic and basic residues (MIFIT2 E156K, MIFIT2 K158E, MIFIT3 E153K, MIFIT3 K156E) were created to potentially disrupt hypothetical salt bridge interactions to break MIFIT2/3 dimerization. For example, mutant basic MIFIT2 E156K may not be able to interact with WT basic MIFIT3 K156. To potentially restore hypothetical salt bridge interactions, double mutants were created. In this double mutant salt bridge model, MIFIT2 E156K was predicted to interact with MIFIT3 K156E while MIFIT2 K158E was predicted to interact with MIFIT3 E153K. The antiviral activity of single and double MIFIT2 and MIFIT3 mutants was analyzed in SFV reporter assays and THOV minireplicon assays.

In SFV reporter assays, WT IFIT2/3 co-expression leads to significantly lower reporter expression than the positive control (100% SFV reporter output) (Figs. 7A & 7B). However, co-transfection of single MIFIT2 mutants with WT and mutant MIFIT3 does not result in significantly lower fluorescence (Fig. 7A). Co-transfection of single MIFIT3 mutants

with WT and mutant MIFIT2 also does not result in significantly lower outputs (Fig. 7B). These data indicate that mutating key acidic and basic residues in subdomain 2 of MIFIT2 and MIFIT3 leads to less antiviral activity against the SFV reporter system than WT IFIT2/3. Double mutants (MIFIT2 E156K K158E and MIFIT3 E153K K156E) co-expressed to potentially restore hypothetical salt bridge interactions had reporter outputs similar to those of the single mutants, suggesting that these residues may not interact via salt bridges to restore IFIT2/3 antiviral activity.

In the THOV minireplicon assay, many of the luminescence outputs of mutant MIFIT2/3 heterodimers are statistically different from the reporter outputs of the positive control (100% viral output) and WT IFIT2/3 (Figs. 7C & 7D). These data indicate that mutating key acidic and basic residues in subdomain 2 of MIFIT2 and MIFIT3 results in reduced, but not inhibited, MIFIT2/3 antiviral activity.

3.3 IFIT2/3 Recombination Model

The IFIT2/3 recombination model is based on the gene recombination signature of IFIT2 and IFIT3. Recurrent rearrangement between the two proteins indicates that IFIT2 and IFIT3 may interact and cofunction, suggesting that this recombination site may also be an IFIT2/3 dimerization site. In this model (Fig. 8), IFIT2 and IFIT3 are inverted on top of each other such that their recombination regions can interact. Point mutations along the recombining helices (MIFIT2 Q72A, MIFIT2 G75K, MIFIT2 S111A, MIFIT2 S111A-D118A, MIFIT3 D79T, MIFIT3 S83A, MIFIT3 S111A, MIFIT3 A115T, MIFIT3 Q122K) were created to test the functionality and interaction of the recombination site. We chose residues that are surface exposed and face away from any RNA-binding surfaces described in all IFIT structures. When possible, the mutated residue was changed to an amino acid at the

corresponding position in IFIT1 to mitigate the possibility of disrupting protein structure or RNA binding.

In SFV reporter assays, the fluorescence outputs of MIFIT2 S111A with both WT MIFIT3 and mutant MIFIT3 are statistically higher than the fluorescence outputs of WT MIFIT2/3 (Figs. 9A & 9B), indicating loss of WT antiviral function. Reduced SFV reporter outputs in MIFIT2 S111A-associated heterodimers also suggest that S111 is a key residue involved in MIFIT2/3 antiviral activity. Importantly, in HIFIT1, the homologous position is an alanine, suggesting that an alanine at this position is compatible with RNA binding and antiviral function. Other mutations within this recombination region (MIFIT2 Q72A, MIFIT2 G75K, MIFIT2 S111A-D118A, MIFIT3 D79T, MIFIT3 S83A, MIFIT3 S111A, MIFIT3 A115T, MIFIT3 Q122K did not significantly reduce fluorescence in the SFV reporter assay (Figs. 9A & 9B). This indicates that only certain amino acids along the recombination region are critical for MIFIT2/3 antiviral activity.

DISCUSSION

4.1 IFIT2/3 Heterodimer: Antiviral Activity

Many innate immunity proteins sense foreign RNA modifications and structures, initiating downstream pathways that inhibit pathogenesis (Fensterl & Sen, 2015; Fleith et al., 2018; Loo & Gale, 2011; Reikine et al., 2014). For example, IFITs are a group of ISGs with helix-turn-helix TPRs known to mediate protein-protein (Abbas et al., 2013) and protein-RNA (Diamond, 2014) interactions. Extensive research has been conducted on MIFIT1B, an ISG that identifies cap0 viral RNA to inhibit translation of viral proteins (Fensterl & Sen, 2015). Contrastingly, HIFIT1 is able to restrict viruses that produce cap1-mRNAs (Daugherty et al., 2016). Little is known about the antiviral mechanisms of other IFIT proteins like IFIT2 and IFIT3.

Structural analysis reveals that IFIT2 and IFIT3 share a conserved region in subdomain 1 that undergoes recurrent recombination (Daugherty, unpublished data). This frequent exchange of genetic material suggests that IFIT2 and IFIT3 likely interact with each other, oligomerize with pathogen-derived RNA (Daugherty & Malik, 2012), and coevolve due to implied cofunction.

Co-immunoprecipitation (Co-IP) experiments demonstrate that IFIT2 and IFIT3 consistently interact with each other and RNA (Agustina D'Urso, unpublished data), corroborating the idea that IFIT2 and IFIT3 heterodimerize for cofunction against viral RNA. Indeed, IFIT2/3 antiviral activity is evident in several viral reporter assays. For example, in SFV assays, WT MIFIT2/3 reporter outputs are significantly less than 100% (positive control), indicating that WT MIFIT2/3 heterodimers have antiviral function (Fig. 5A). MIFIT2/3 antiviral activity in SFV reporter systems is corroborated by MIFIT2/3-mediated

viral inhibition against Sindbis virus (Candace Todd, unpublished data), a similar *Alphavirus* with a positive sense, single-stranded RNA genome virus (Suhrbier et al., 2012). It is important to note that the HIFIT data trends towards heterodimer-mediated antiviral activity (Fig. 5B) but is not as defined as the MIFIT data. In SFV assays, HIFIT2, HIFIT3, and HIFIT2/3 generally have higher reporter outputs, greater variability, and weaker antiviral effects than MIFIT2, MIFIT3, and MIFIT2/3 (Figs. 5A & 5B).

The same trend is evident in THOV assays. MIFIT2/3 displays significant antiviral activity against the THOV reporter system (Fig. 5C) while HIFIT2/3 has a similar, but subtler, effects (Fig. 5D). However, in both cases, the IFIT2/3 heterodimers appear to have more antiviral activity than IFIT2 alone and IFIT3 alone. These data indicate that IFIT2/3 antiviral function is markedly different from that of MIFIT1B and HIFIT1 which can act as singular effector molecules.

Indeed, antiviral functional analysis in the IAV minireplicon system provides further evidence that IFIT2/3 antiviral mechanisms are distinct from those of MIFIT1B. IAV utilizes a "cap-snatching" mechanism such that its mRNAs have 5' ends derived from host cell pre-mRNAs (Burgui et al., 2007). Without pathogen-derived cap0 mRNA, IAV is able to evade MIFIT1B recognition and subsequent inhibition. However, IAV reporter assay data suggest that MIFIT2/3 is able to inhibit IAV infection (Fig. 5E). It follows that IFIT2/3 must employ a unique antiviral mechanism that does not solely rely on viral mRNA 5' cap recognition. Further analysis of the isolated viral RNA from IFIT2/3 Co-IP experiments will help identify IFIT2/3-susceptible RNAs distinct from those targeted by MIFIT1B and HIFIT1.

In addition, MIFIT2/3 significantly reduces viral output in the EBOV minigenome system as indicated by decreased firefly luminescence (Fig. 5F). This suggests that MIFIT2/3

is antiviral against EBOV. Further optimization of the EBOV system will allow for a more precise understanding of MIFIT2/3-mediated antiviral activity against EBOV.

4.2 Salt Bridge Model: RNA Binding

The crystal structure of IFIT2 (Yang et al., 2012) suggests that IFIT2 and IFIT3 may dimerize with potential salt bridges in a swapped dimer fashion (Fig. 6C). In our proposed salt bridge model, acidic and basic residues conserved in HIFIT2, HIFIT3, MIFIT2, and MIFIT3 face away from the proposed RNA binding site. Hypothetical salt bridges potentially link these charged groups such that IFIT2 acidic residues may interact with IFIT3 basic residues and vice versa. The potential salt bridges were predicted to mediate potential IFIT2 E156 interaction with IFIT3 K156 and potential IFIT2 K158 interaction with IFIT3 E153. If these proposed salt bridges were critical for dimerization but not RNA binding, mutated IFIT2 and IFIT3 would not dimerize or display antiviral activity like the WT IFIT2/3 dimer.

Indeed, the SFV assay data suggest that MIFIT2/3 antiviral activity is mediated by these charged residues in subdomain 2 of MIFIT2 and MIFIT3. When singular acidic and basic residues on MIFIT2 and MIFIT3 are mutated (MIFIT2 E156K, MIFIT2 K158E, MIFIT3 ME153K, MIFIT3 K156E), reporter outputs are significantly similar to the positive control (Figs. 7A & 7B). This indicates that mutating charged residues in subdomain 2 significantly decreases the ability of MIFIT2/3 to mitigate SFV infection. It follows that MIFIT2 E156, MIFIT2 K158, MIFIT3 E153, and MIFIT3 K156 may all play a role in mediating the antiviral function of the MIFIT2/3 heterodimer.

To potentially restore the antiviral activity and proposed salt bridge interactions between MIFIT2 and MIFIT3, double mutants (MIFIT2 E156K K158E and MIFIT3 E153K K156E) were created. If MIFIT2 and MIFIT3 dimerize at this site, the complete reversal of

acidic and basic residues in both MIFITs would potentially allow for hypothetical salt bridge restoration such that MIFIT2 E156K would interact with MIFIT3 K156E and MIFIT2 K158E would interact with MIFIT3 E153K. However, the beta-galactosidase outputs of these double mutant heterodimers in SFV assays were similar to those of the single mutant heterodimers (Figs. 7A & 7B), indicating lack of antiviral activity.

Since the antiviral activity of WT MIFIT2/3 heterodimers cannot be restored with double mutants in SFV reporter assays, these proposed salt bridges may not actually be critical for IFIT2/3 heterodimerization. However, the acidic and basic residues may play a different role in mediating IFIT2/3 antiviral activity. For example, MIFIT2 E156, MIFIT2 K158, MIFIT3 E153, and MIFIT3 K156 may interact with a foreign entity, like viral RNA, that confers antiviral activity. Mutant MIFIT2 E156, MIFIT2 K158, MIFIT3 E153, and MIFIT3 K156 may lead to high viral reporter outputs in SFV assays because disrupting key residues in subdomain 2 of IFIT2 and IFIT3 may prevent RNA binding. It follows that the acidic and basic residues in subdomain 2 of IFIT2 and IFIT3 may be critical for antiviral function, but not dimerization. Indeed, studies indicate that a positively-charged cavity in subdomain 2 of HIFIT1 interacts with the 5' end of viral mRNA, inhibiting translation (Fensterl & Sen, 2015). If IFIT2 and IFIT3 bind RNA similarly to IFIT1, in subdomain 2, MIFIT2 E156, MIFIT2 K158, MIFIT3 E153, and MIFIT3 K156 may be critical for RNA-mediated antiviral activity.

This hypothesis is supported by THOV minireplicon assay data. In THOV assays, as indicated by higher luminescence levels, mutant acidic and basic residues in MIFITs tend to reduce the antiviral activity of MIFIT2/3 heterodimers (Figs. 7C & 7D). However, mutating the hypothetical MIFIT salt bridges does not appear to consistently and strongly inhibit

IFIT2/3 antiviral function as it did in SFV assays. For instance, many mutant dimers exhibit antiviral activity significantly different from both IFIT2/3 THOV reporter outputs and the positive control (Figs. 7C & 7D). This variance in inhibition levels may have to do with differential binding capabilities for negative-stranded THOV RNA versus positive-stranded SFV RNA. However, it is important to note that both in SFV and THOV assays, mutated charged residues lead to decreased MIFIT2/3 antiviral function, likely due to poor viral RNA binding affinity.

Co-IP experiments were conducted to understand the role of MIFIT salt bridges in heterodimerization versus RNA-binding. Co-IP data indicate that proposed salt bridge mutations weaken, but do not fully disrupt, MIFIT2/3 heterodimerization (Agustina D'Urso, unpublished data) (Fig. 7E). Since MIFIT2 E156K, MIFIT2 K158E, MIFIT3 E153K, MIFIT3 K156E do not knock out MIFIT2/3 interaction, it is likely that these acidic and basic amino acids are not necessary for dimerization. Indeed, when WT and mutant MIFIT2/3 samples are treated with RNase prior to pull-down, interaction still occurs (Agustina D'Urso, unpublished data). These data again suggest that the RNA binding domain and the dimerization domain of MIFIT2 and MIFIT3 are unique entities. It follows that MIFIT2 E156, MIFIT2 K158, MIFIT3 E153, and MIFIT3 K156 in subdomain 2 may be critical for RNA binding, but not protein heterodimerization.

4.3 Recombination Model: Heterodimerization

Therefore, a new heterodimer model (Fig. 8) was generated to identify the dimerization site between MIFIT2 and MIFIT3. This model was established in reference to the gene recombination signature of MIFIT2 and MIFIT3. Recurrent rearrangement at the recombination region of subdomain 1 is an indication of IFIT2/3 pathogen-mediated

antagonism (Daugherty & Malik, 2012). Because this recombination site likely undergoes coevolution with a pathogen, it may be also be a dimerization region—a point at which IFIT2 and IFIT3 may interact and evolve in response to viral RNA.

Indeed, data indicate that MIFIT2/3 antiviral activity is mediated by the predicted recombination region in subdomain 1 of IFIT2 and IFIT3. SFV assay data indicate that when MIFIT2 S111 along the recombining TPR is mutated, reporter outputs are significantly higher than those of WT IFIT2/3 (Figs. 9A & 9B). This indicates that disrupting amino acids in the recombination region of MIFIT2 decreases the antiviral activity of IFIT2/3. It follows that MIFIT2 S111 may play a role in antiviral function by mediating heterodimerization.

This hypothesis is supported by Co-IP experiments which indicate that MIFIT2 S111A does not interact with WT or mutant MIFIT3 (Agustina D'Urso, unpublished data) (Fig. 9C). Since MIFIT2 S11A potentially disrupts IFIT2/3 interaction, it may be said that the recombination region of MIFIT2 contributes to IFIT2/3 antiviral activity by mediating heterodimerization between the two molecules.

It is also important to note that not all mutations along the recombining region of MIFIT2 and MIFIT3 (MIFIT2 Q72A, MIFIT2 G75K, MIFIT2 S111A-D118A, MIFIT3 D79T, MIFIT3 S83A, MIFIT3 S111A, MIFIT3 A115T, MIFIT3 Q122K) inhibit heterodimerization. These mutations did not disrupt MIFIT2/3 interaction in Co-IP experiments (Agustina D'Urso, unpublished data) (Fig. 9C) or result in SFV reporter outputs that were significantly higher than those of WT MIFIT2/3. This suggests that not all residues within the recombining region of subdomain 1 of MIFIT2 and MIFIT3 are critical for heterodimerization and subsequent MIFIT2/3-mediated antiviral function.

4.4 IFIT2/3 Antiviral Activity: RNA Binding and Heterodimerization

The antiviral activity of IFIT2/3 indicates that IFIT mechanisms are unique and complex. Rather than acting as individual effector proteins like MIFIT1B and HIFIT1, IFIT2 and IFIT3 heterodimerize to exhibit antiviral function against a broad range of viruses.

When acidic and basic residues in subdomain 2 of MIFIT2 and MIFIT3 are mutated (MIFIT2 E156K, MIFIT2 K158E, MIFIT3 E153K, MIFIT3 K156E), MIFIT2/3 antiviral activity in SFV and THOV is inhibited at various levels (Fig. 7). These data testify to the functional significance of these charged residues. However, Co-IP experiments indicate that mutated charged residues on MIFIT2 and MIFIT3 do not disrupt MIFIT2/3 interaction (Agustina D'Urso, unpublished data) (Fig. 7E). It follows that MIFIT2 E156K, MIFIT2 K158E, MIFIT3 E153K, and MIFIT3 K156E are critical for antiviral functionality but not oligomerization. This antiviral function is likely due to RNA binding.

SFV data also indicate that mutating the recombination region of subdomain 1 in MIFIT2 (MIFIT2 S111A) also inhibits the antiviral activity of MIFIT2/3 (Fig. 9). Co-IP experiments demonstrate that this mutation also breaks interaction between MIFIT2 and MIFIT3 (Agustina D'Urso, unpublished data) (Fig. 9C). These findings indicate that the recombination region in subdomain 1 of MIFIT2 may be a dimerization site.

However, since viral reporter assays and Co-IP experiments are artificial systems, these data do not fully explain the MIFIT2/3 antiviral mechanism. To corroborate viral reporter assay results via live viral infection, stable cell lines that constitutively express WT and mutant IFIT2 and IFIT3 have been created. Numerous viruses related to SFV, THOV, IAV, and EBOV may also be tested in these cell lines to obtain a broad understanding of the types of pathogens IFIT2/3 may inhibit. In addition, pull-down assays of IFIT2 and IFIT3 in a bacterial expression system will confirm the IFIT2/3 interaction data from Co-IP experiments.

Reverse transcription PCR of the RNA from these pull-downs will help specify what RNA sequences and regions IFIT2/3 recognizes. Finally, analysis of new mutations along the proposed RNA binding helix and recombining dimerization site will corroborate initial findings and further identify the key amino acids involved with IFIT2/3 RNA binding and heterodimerization.

In conclusion, the antiviral activity of IFIT2/3 is mediated by two components: RNA binding and heterodimerization. Acidic and basic amino acid residues (MIFIT2 E156, MIFIT2 K158, MIFIT3 E153, MIFIT3 K156) in subdomain 2 of MIFIT2 and MIFIT3 convey RNA binding function while the recombination region of subdomain 1 may function as a dimerization site via MIFIT2 S111. Understanding the antiviral mechanisms of this heterodimer through RNA binding will elucidate how IFIT proteins prevent viral replication and help predict which pathogens may be inhibited by IFIT2/3 dimers. In addition, analysis of IFIT2/3 heterodimerization will provide insights into the mechanisms of host innate immune response in regards to protein interaction and antiviral activity.

FIGURES

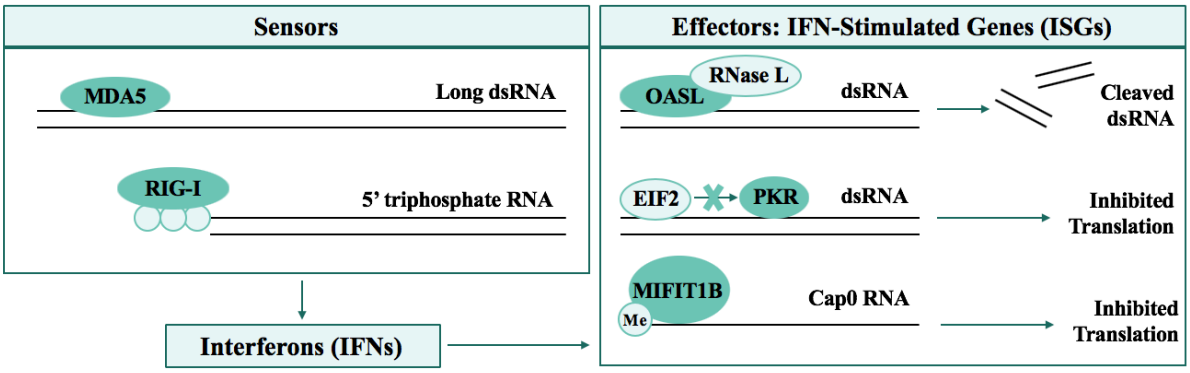

Figure 1. Defense strategies employed by the host innate immune system against foreign RNA. The host innate immune system is comprised of sensors and effectors which target specific viral RNA sequences, structures, and modifications. MDA5 is an innate immune receptor that recognizes long viral dsRNA. RIG-I is an innate sensor that identifies the 5'-triphosphate caps of viral dsRNA. Innate immune system effectors recognize viral RNA, initiating signaling cascades that activate broad antiviral responses against pathogens. For example, OASL recognizes exogenous nucleic acids and activates RNase L, cleaving viral transcripts. PKR is an effector that blocks translation when bound to foreign dsRNA. MIFIT1B targets cap0 RNA, inhibiting translation of viral proteins.

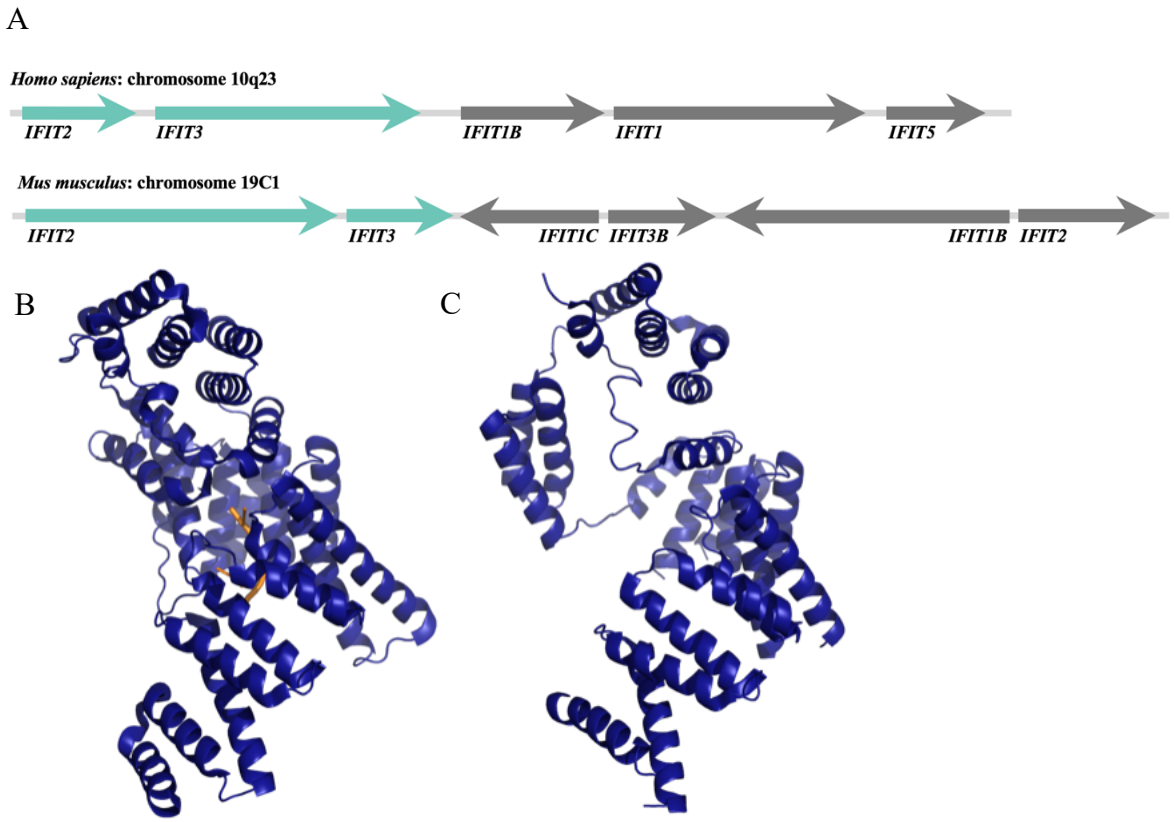

Figure 2. Gene organization and structure of IFITs. (A) Human and mouse IFIT locus. The exon structures are denotated with arrows while introns are indicated by the grey bar. Of note are IFIT2 and IFIT3, which will be the focus of this paper. (B) The RNA-bound human IFIT1 (HIFIT1) structure depicts a compact RNA binding pocket. (C) The IFIT2 structure contains a predicted nucleotide-binding channel similar to that of HIFIT1.

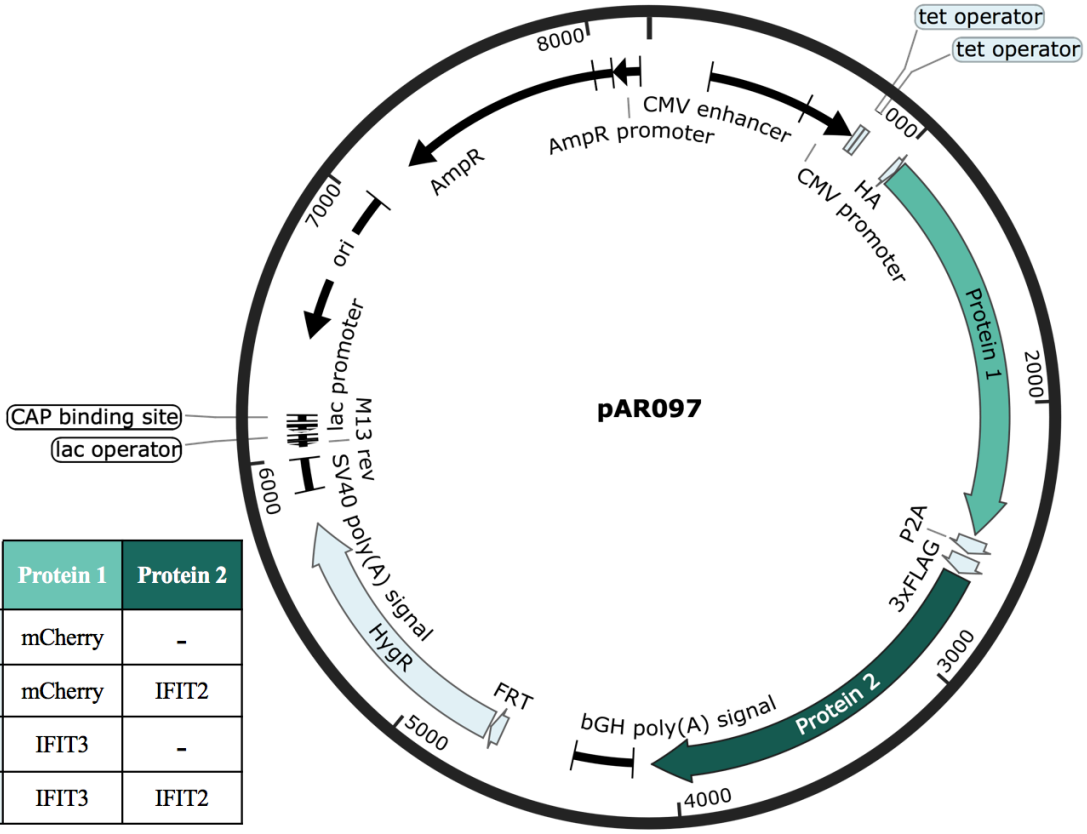

	Protein 1	Protein 2
Empty	mCherry	-
IFIT2	mCherry	IFIT2
IFIT3	IFIT3	-
IFIT2/3	IFIT3	IFIT2

Figure 3. Multicistronic expression vector pAR097 (created via SnapGene). The self-cleaving P2A site allows for co-expression of two proteins. Empty vector expresses mCherry, IFIT2 vector co-expresses mCherry and IFIT2, IFIT3 vector expresses IFIT3, and IFIT2/3 vector co-expresses IFIT3 and IFIT2. Ampicillin resistance allows for selection of successful pAR097 clones. pAR097 may also be used to generate dox-inducible stable cell lines (FRT site) selected for based on hygromycin resistance.

Figure 4. Viral reporter systems utilized to evaluate IFIT-mediated antiviral response. (A) Viral reporter assays were used to quantify IFIT-mediated antiviral activity. The basic premise behind the systems used in this paper was to transfect viral non-structural protein plasmid(s) and a viral reporter plasmid into 293T cells. These non-structural proteins would then synthesize a viral polymerase to transcribe the reporter mRNA. This would allow for the quantification of viral reporter expression with and without IFITs. (B) The pSMART vector produces Semliki Forest Virus (SFV) non-structural proteins which make a viral polymerase that increases lacZ expression, producing beta-galactosidase. Beta-galactosidase cleaves 4-methylumbelliferyl-β-D-galactopyranoside (4-MUG), generating a fluorophore which is monitored by a fluorescent plate reader. (C) Viral polymerase plasmids specific for thogoto virus (THOV), influenza A virus (IAV), and ebola virus (EBOV) synthesize a viral polymerase which transcribes a reporter (firefly luciferase) gene flanked by viral UTRs mimics viral expression. Firefly luciferase production can be monitored by a plate reader.

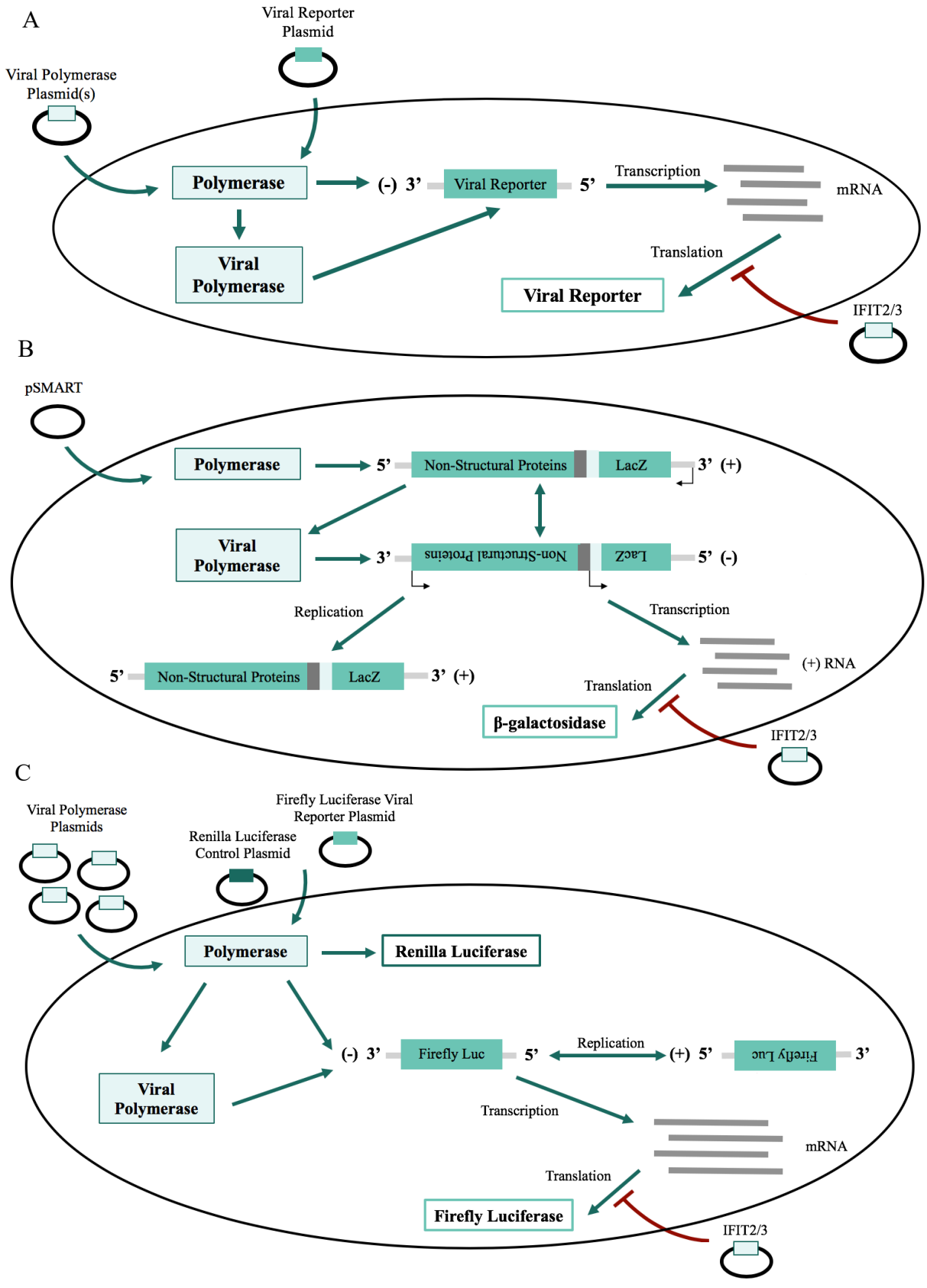
A
Viral Reporter Plasmid
Viral Polymerase Plasmid(s)
Polymerase
(-) 3'
Viral Reporter
5'
Transcription
mRNA
Viral Polymerase
Translation
Viral Reporter
IFIT2/3
B
pSMART
Polymerase
5'
Non-Structural Proteins
LacZ
3' (+)
Viral Polymerase
3'
Non-Structural Proteins
LacZ
5' (-)
Replication
Transcription
5'
Non-Structural Proteins
LacZ
3' (+)
(+) RNA
Translation
β-galactosidase
IFIT2/3
C
Viral Polymerase Plasmids
Firefly Luciferase Viral Reporter Plasmid
Renilla Luciferase Control Plasmid
Polymerase
Renilla Luciferase
(-) 3'
Firefly Luc
5'
Replication
(+) 5'
Firefly Luc
3'
Viral Polymerase
Transcription
mRNA
Translation
Firefly Luciferase
IFIT2/3

Figure 5. WT IFIT2/3 heterodimer antiviral activity in viral reporter systems. All positive controls (empty transfection) were done in triplicate or quadruplicate and normalized to 100% viral output. All experimental conditions were done in triplicate. (A) MIFIT2/3 and (B) HIFIT2/3) heterodimers result in significantly lower semliki forest virus (SFV) viral expression than the positive control, IFIT2 alone, and IFIT3 alone. These data indicate that IFIT2/3 heterodimers have antiviral activity in SFV reporter assays. (C) MIFIT2/3 and (D) HIFIT2/3 heterodimers result in significantly lower thogoto virus (THOV) viral expression than the positive control, indicating that IFIT2/3 heterodimers have antiviral activity in the THOV minigenome system. (E) The MIFIT2/3 heterodimer results in significantly lower influenza A virus (IAV) viral expression than the positive control, indicating that MIFIT2/3 has antiviral activity in the IAV minigenome system. (F) MIFIT2/3 significantly reduces ebola virus (EBOV) output when compared to positive control reporter expression, indicating MIFIT2/3-mediated antiviral activity in the EBOV minigenome system.

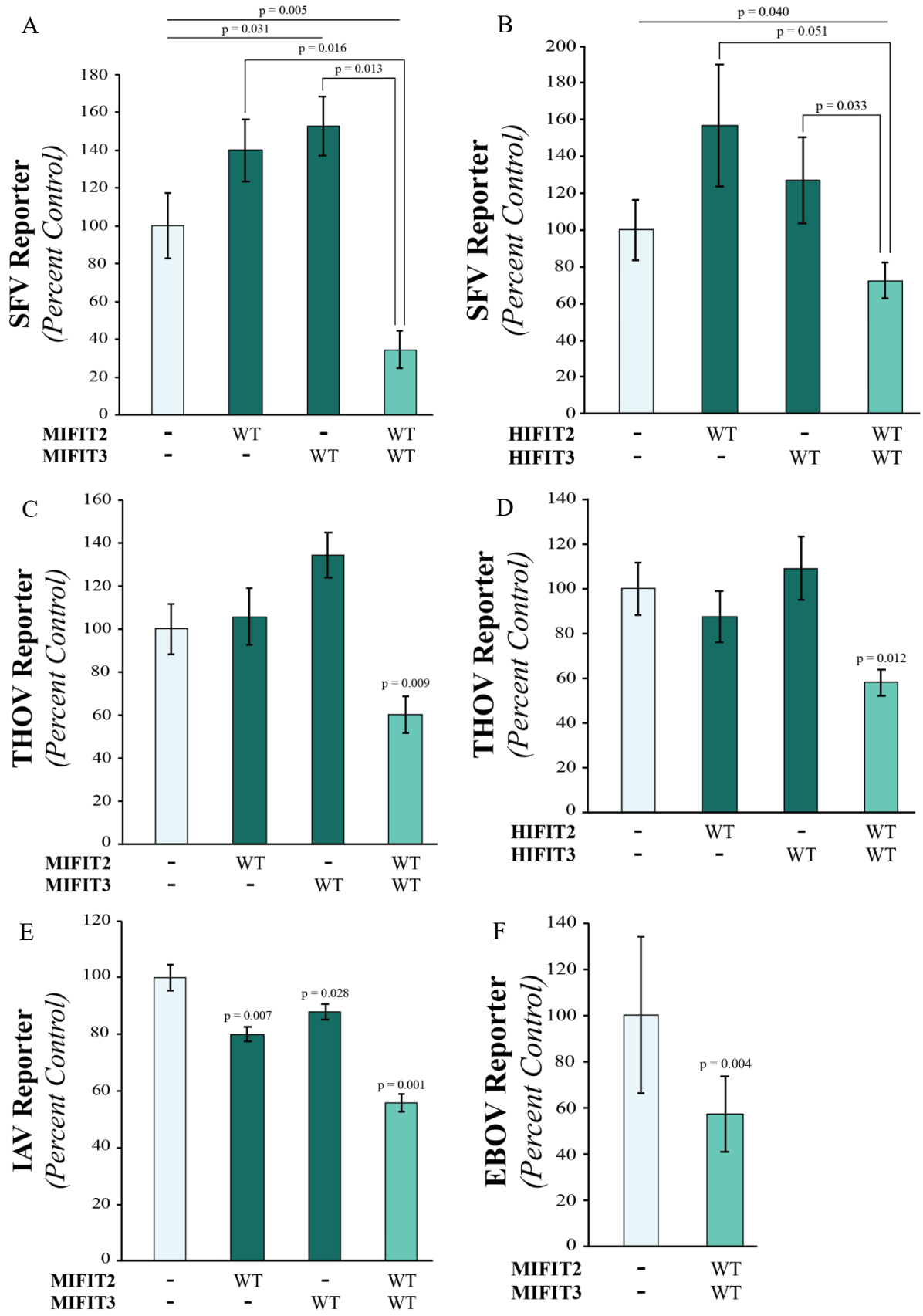
A
SFV Reporter
(Percent Control)
p = 0.005
p = 0.031
p = 0.016
p = 0.013
MIFIT2 - WT - WT
MIFIT3 - - WT WT
B
SFV Reporter
(Percent Control)
p = 0.040
p = 0.051
p = 0.033
HIFIT2 - WT - WT
HIFIT3 - - WT WT
C
THOV Reporter
(Percent Control)
p = 0.009
MIFIT2 - WT - WT
MIFIT3 - - WT WT
D
THOV Reporter
(Percent Control)
p = 0.012
HIFIT2 - WT - WT
HIFIT3 - - WT WT
E
IAV Reporter
(Percent Control)
p = 0.007
p = 0.028
p = 0.001
MIFIT2 - WT - WT
MIFIT3 - - WT WT
F
EBOV Reporter
(Percent Control)
p = 0.004
MIFIT2 - WT
MIFIT3 - WT

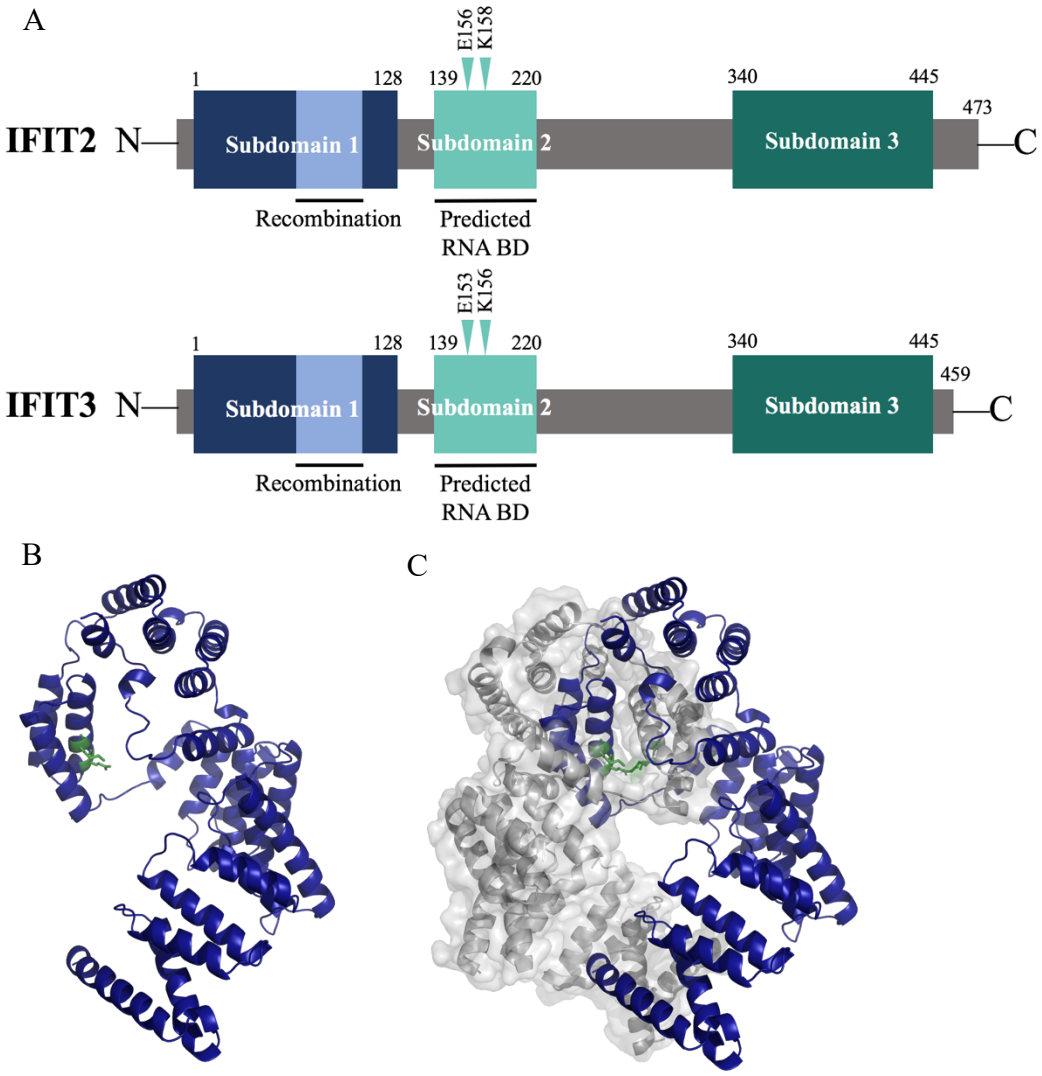

Figure 6. IFIT2/3 salt bridge heterodimer model. (A) IFIT2 and IFIT3 predicted protein domains. Subdomain 2 (139 – 220 AA) may interact with viral RNA, proving critical to IFIT2 and IFIT3 antiviral function. Because IFIT2 and IFIT3 cofunction (Figure 5), this region may also be critical to IFIT2/3 heterodimerization. Therefore, point mutations to acidic and basic residues (MIFIT2 E156K, MIFIT2 K158E, MIFIT3 E153K, MIFIT3 K156E) were created along this potential RNA-binding region as indicated by the green triangles. (B) Proposed IFIT2 structure with green amino acid residues indicating point mutations. (C) Proposed IFIT2/3 heterodimerization in which MIFIT2 E156 interacts with MIFIT3 K156 and MIFIT2 K158 interacts with MIFIT3 E153. These putative salt bridges (green) were mutated to disrupt potential IFIT2/3 heterodimerization at this site.

Figure 7. IFIT2/3 heterodimer antiviral activity is mediated by the predicted RNA binding region of subdomain 2. Point mutations to acidic and basic residues along the potential RNA-binding region (MIFIT2 E156K, MIFIT2 K158E, MIFIT3 E153K, MIFIT3 K156E) disrupted viral reporter activity, indicating the functional significance of these residues. All positive controls (empty transfection) were done in triplicate or quadruplicate and normalized to 100% viral output. All experimental conditions were done in triplicate. (A) Mutant MIFIT2 with WT and mutant MIFIT3 and (B) mutant MIFIT3 with WT and mutant MIFIT2 lead to semliki forest virus (SFV) reporter outputs similar to that of the positive control, not that of WT MIFIT2/3 (summarized in (E)). Similarly, (C) mutant MIFIT2 with WT and mutant MIFIT3 and (D) mutant MIFIT3 with WT and mutant MIFIT2 lead to thogoto virus (THOV) reporter outputs different from both that of the positive control and that of WT MIFIT2/3 (summarized in (E)). These data suggest that MIFIT2 E156, MIFIT2 K158, MIFIT3 E153, and MIFIT3 K156 are critical for the antiviral activity of IFIT2/3 as observed in SFV and THOV reporter assays. However, these amino acids may not be critical for IFIT2/3 heterodimerization, as indicated by co-immunoprecipitation data (E) which suggests that despite charged residue mutations, IFIT2 and IFIT3 still interact.

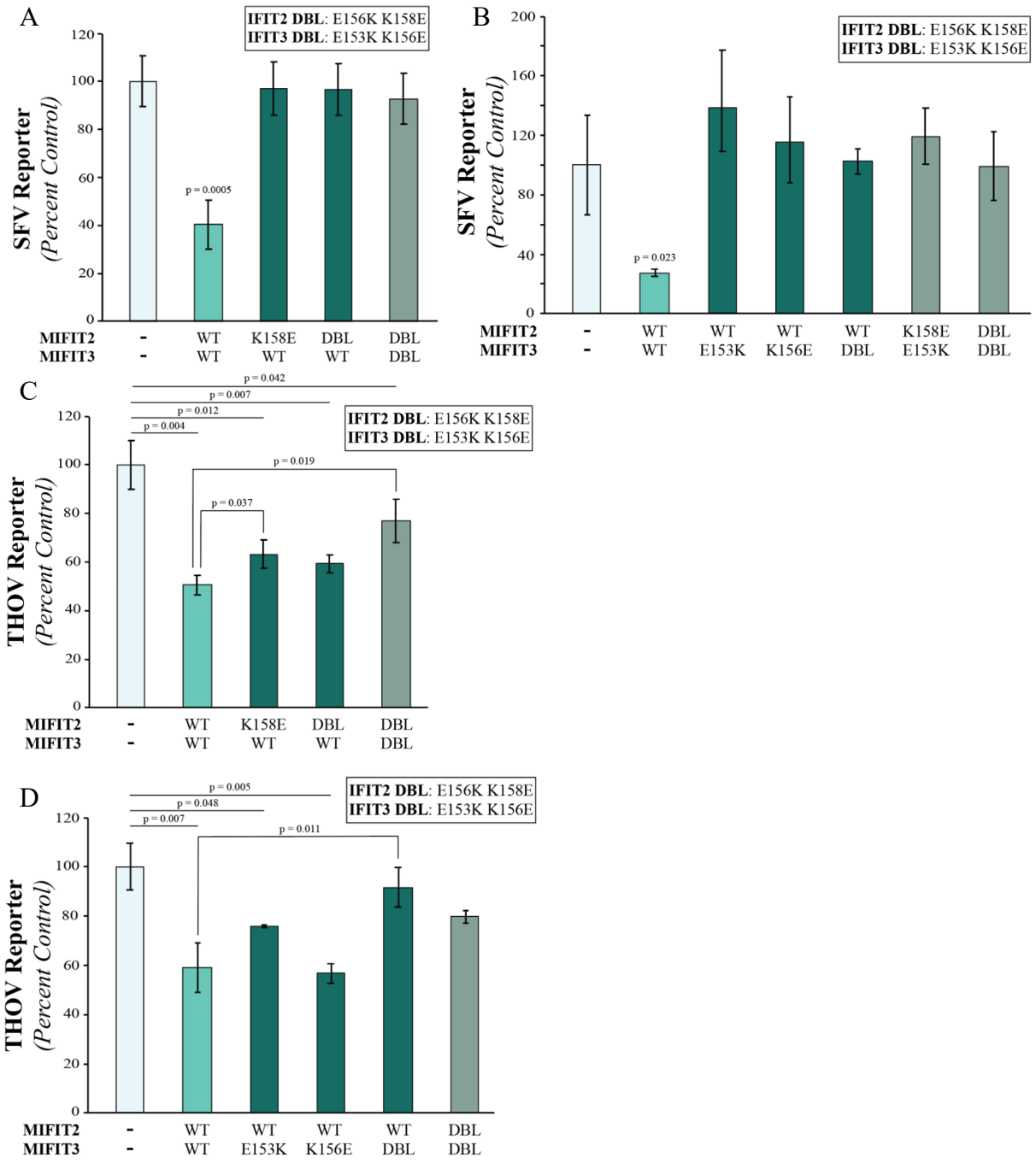

E

MIFIT2	WT	K158E	E156K K158E	WT	WT	WT	E156K K158E
MIFIT3	WT	WT	WT	E153K	K156E	E153K K156E	E153K K156E
SFV Reporter Output	34.11%	96.91%	96.63%	137.79%	115.54%	102.45%	95.98%
THOV Reporter Output	56.62%	63.15%	59.25%	75.81%	56.82%	91.70%	76.94%
Co-IP Interaction*	✓	✓	✓	✓	✓	✓	✓

*Unpublished data by Dr. Agustina D'Urso

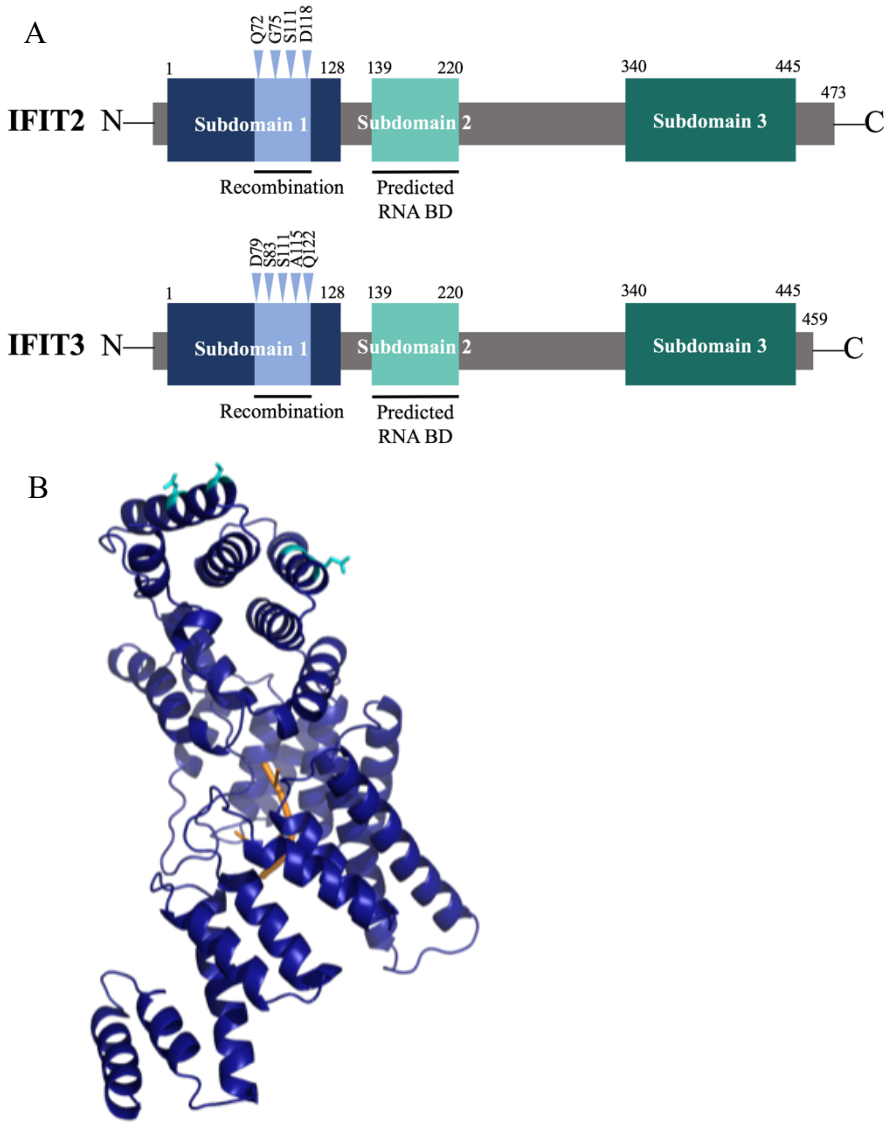

Figure 8. IFIT2/3 recombination heterodimer model. (A) IFIT2 and IFIT3 predicted protein domains. Subdomain 1 (1 – 128 AA) is highly homologous, with a small region undergoing recurrent recombination. Point mutations (MIFIT2 Q72A, MIFIT2 G75K, MIFIT2 S111A, MIFIT2 S111A D118A, MIFIT3 D79A, MIFIT3 S83A, MIFIT3 S111A, MIFIT3 A115T, MIFIT3 Q122K) were created along this recombining region as indicated by blue triangles. Mutations at this site were predicted to disrupt the proposed IFIT2/3 heterodimer structure interacting at the recombining region of subdomain 1. (B) IFIT2 structure modeled onto the human IFIT1 (HIFIT1) structure to accommodate for the proposed RNA-binding region. Blue amino acid residues indicate which point mutants were created to disrupt IFIT2/3 interaction. viral reporter output of the IFIT2 S111A and IFIT3 S83A heterodimer and the IFIT2 S111A and IFIT3 T115A heterodimer was significantly higher than that of the WT IFIT2/3 heterodimer.

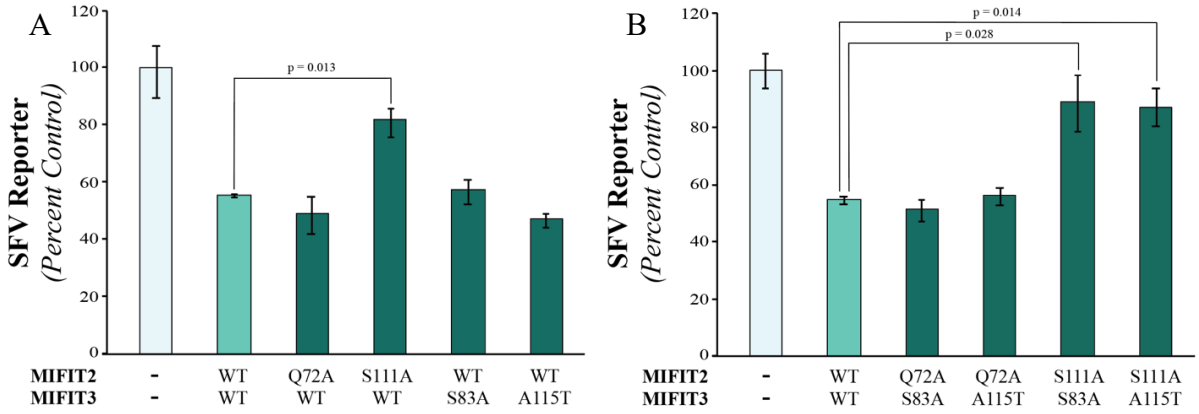

C

MIFIT2	Q72A	S111A	WT	WT
MIFIT3	WT	WT	S83A	A115T
SFV Reporter Output	48.88%	81.87%	57.33%	47.05%
Co-IP Interaction*	✓	-	✓	✓

*Unpublished data by Dr. Agustina D'Urso

Figure 9. IFIT2/3 heterodimer antiviral activity is mediated by the predicted recombination region of subdomain 1. S111A along the recombination region of MIFIT2 disrupts semliki forest virus (SFV) viral reporter activity, indicating the functional significance of this residue. Other mutations along the potential recombination region (MIFIT2 Q72A, MIFIT3 S83A, MIFIT3 S111A, MIFIT3 A115T) did not disrupt SFV viral reporter activity. (A) Mutant MIFIT2 with WT MIFIT3 and mutant MIFIT3 with WT MIFIT2 SFV viral reporter outputs indicate that MIFIT2 S111A disrupts WT IFIT2/3-mediated antiviral activity. (B) Mutant IFIT2 and mutant IFIT3 co-expression data also indicates that MIFIT2 S111A heterodimers have higher viral reporter outputs than WT IFIT2/3. MIFIT2 S111A may be critical for IFIT2/3 heterodimerization, as indicated by co-immunoprecipitation data (C) which suggests that mutating this residue inhibits IFIT2/3 interaction.

REFERENCES

Abbas, Y. M., Laudenbach, B. T., Martínez-Montero, S., Cencic, R., Habjan, M., Pichlmair, A., Damha, M. J., Pelletier, J., & Nagar, B. (2017). Structure of human IFIT1 with capped RNA reveals adaptable mRNA binding and mechanisms for sensing N1 and N2 ribose 2'-O methylations. *Proceedings of the National Academy of Sciences of the United States of America*, *114*(11), E2106-15. doi: 10.1073/pnas.1612444114

Abbas, Y. M., Pichlmair, A., Górna, M. W., Superti-Furga, G., & Nagar, B. (2013). Structural basis for viral 5'-PPP-RNA recognition by human IFIT proteins. *Nature*, *494*(7435), 60-4. doi: 10.1038/nature11783

Ahola, T., Lampio, A., Auvinen, P., & Kääriäinen, L. (1999). Semliki forest virus mRNA capping enzyme requires association with anionic membrane phospholipids for activity. *The EMBO Journal*, *18*(11), 3164-72. doi: 10.1093/emboj/18.11.3164

Burgui, I., Yángüez, E., Sonenberg, N., & Nieto, A. (2007). Influenza virus mRNA translation revisited: is the eIF4E cap-binding factor required for viral mRNA translation?. *Journal of Virology*, *81*(22), 12427-38. doi: 10.1128/JVI.01105-07

Centers for Disease Control and Prevention. (2018, December 17). *Chikungunya virus.* https://www.cdc.gov/chikungunya/index.html.

Choi, U. Y., Kang, J. S., Hwang, Y. S., Kim, Y. J. (2015). Oligoadenylate synthase-like (OASL) proteins: dual functions and associations with disease. *Experimental & Molecular Medicine, 5,* e144. doi: 10.1038/emm.2014.110

Cressey, T. (2016, March 17). *Minigenomes— a safe way to study dangerous viruses.* https://blog.addgene.org/minigenomes-a-safe-way-to-study-dangerous-viruses

Daffis, S., Szretter, K. J., Schriewer, J., Li, J., Youn, S., Errett, J, Lin, T., Schneller, S., Zust, R., Dong, H., Thiel, V., Pierson, T. C., Buller, R. M., Gale, M., Shi, P., Diamond, M. S. (2010). 2'-O methylation of the viral mRNA cap evades host restriction by IFIT family members. *Nature*, *468*(7322), 452–456. doi:10.1038/nature09489

Daugherty, M. D., & Malik, H. S. (2012). Rules of engagement: molecular insights from host-virus Arms races. *Annual Review of Genetics, 46*, 677-700. doi: 10.1146/annurev-genet-110711-155522

Daugherty, M. D., Schaller, A. M., Geballe, A. P., & Malik, H. S. (2016). Evolution-guided functional analyses reveal diverse antiviral specificities encoded by IFIT1 genes in mammals. *eLife*, *5*, e14228. doi:10.7554/eLife.14228

Diamond, M. S. (2014). IFIT1: A dual sensor and effector molecule that detects non-2'-O methylated viral RNA and inhibits its translation. *Cytokine & Growth Factor Reviews*, *25*(5), 543-50. doi: 10.1016/j.cytogfr.2014.05.002

DiCiommo, D. P., Duckett, A., Burcescu, I., Bremner, R., & Gallie, B. L. (2004). Retinoblastoma protein purification and transduction of retina and retinoblastoma cells using improved alphavirus vectors. *Innovative Ophthalmology & Visual Science, 45*(9), 3320-29. doi: 10.1167/iovs.04-0140

Dietzgen, R. G., Kondo, H., Goodin, M. M., Kurath, G., & Vasilakis, N. (2016). The family Rhabdoviridae: mono- and bipartite negative-sense RNA viruses with diverse genome organization and common evolutionary origins. *Virus research*, *227*, 158-170. doi: 10.1016/j.virusres.2016.10.010

Fan, M. (2014, September 9). *Plasmids 101: Multicistronic Vectors.* https://blog.addgene.org/plasmids-101-multicistronic-vectors

Fensterl, V., & Sen, G. C. (2015). Interferon-induced IFIT proteins: their role in viral pathogenesis. *Journal of Virology*, *89*(5), 2462-8. doi: 10.1128/JVI.02744-14

Fleith, R. C., Mears, H. V., Leong, X. Y., Sanford, T. J., Emmott, E., Graham, S. C., Mansur, D. S., & Sweeney, T. R. (2018). IFIT3 and IFIT2/3 promote IFIT1-mediated translation inhibition by enhancing binding to non-self RNA. *Nucleic Acids Research*, *46*(10), 5269-5285. doi: 10.1093/nar/gky191

G-Biosciences (2019). *Fluorescent B Galactosidase Assay (MUG)*. https://www.gbiosciences.com/Bioassays/Fluorescent-Galactosidase-Assay-MUG

García, M. A., Gil, J., Ventoso, I., Guerra, S., Domingo, E., Rivas, C., & Esteban, M. (2006). Impact of protein kinase PKR in cell biology: from antiviral to antiproliferative action. *Microbiology and Molecular Biology Reviews*, *70*(4), 1032-60. doi: 10.1128/MMBR.00027-06

Invitrogen (2010, November 9). Flp-In^{Tm} System. https://www.thermofisher.com/document-connect/document-connect.html?url=https%3A%2F%2Fassets.thermofisher.com%2FTFS-Assets%2FLSG%2Fmanuals%2Fflpinsystem_man.pdf&title=RmxwLUluIFN5c3RlbQ==

Loo, Y. M., & Gale, M. (2011). Immune signaling by RIG-I-like receptors. *Immunity*, *34*(5), 680-92. doi: 10.1016/j.immuni.2011.05.003

Mears, H.V., & Sweeney T.R. (2018). Better together: the role of IFIT protein-protein interactions in the antiviral response. *Journal of General Virology, 99*(11): 1463-77. doi: 10.1099/jgv.0.001149

Mogensen, T. H. (2009). Pathogen recognition and inflammatory signaling in innate immune defenses. *Clinical Microbiology Reviews*, *22*(2), 240-73. doi: 10.1128/CMR.00046-08

Mühlberger, E. (2007). Filovirus replication and transcription. *Future Virology*, *2*(2), 205-15. doi: 10.2217/17460794.2.2.205

Pichlmair, A., Lassnig, C., Eberle, C.A., Górna, M.W., Baumann, C.L., Burkard, T.R., Bürckstümmer, T., Stefanovic, A., Krieger, S., Bennett, K.L., Rülicke, T., Weber, F., Colinge,, J., Müller, M, & Superti-Furga, G. (2011). IFIT1 is an antiviral protein that recognizes 5'-triphosphate RNA. *Nature Immunology, 12*(7): 624-30. doi: 10.1038/ni.2048

Promega. (2015 September). *Dual-Glo® luciferase assay system technical manual*. https://www.promega.com/-/media/files/resources/protocols/technical-manuals/0/dual-glo-luciferase-assay-system-protocol.pdf?la=en

Reikine, S., Nguyen, J. B., & Modis, Y. (2014). Pattern recognition and signaling mechanisms of RIG-I and MDA5. *Frontiers in Immunology*, *5*, 342. doi:10.3389/fimmu.2014.00342

Schaefer, M., Kapoor, U., & Jantsch, M. F. (2017). Understanding RNA modifications: the promises and technological bottlenecks of the 'epitranscriptome'. *Open Biology*, *7*(5), 170077. doi: 10.1098/rsob.170077

Stevaert, A., & Naesens, L. (2016). The influenza virus polymerase complex: an update on its structure, functions, and significance for antiviral drug design. *Medicinal Research Reviews*, *36*(6), 1127-73. doi: 10.1002/med.21401

Su, J., Dou, Y., You, Y., & Cai, X. (2015). Application of minigenome technology in virology research of the Paramyxoviridae family. *Journal of Microbiology, Immunology and Infection, 48*(2), 123-9. doi: 10.1016/j.jmii.2014.02.008

Suhrbier, A., Jaffar-Bandjee, M., & Gasque, P. (2012). Arthritogenic alphaviruses—an overview. *Nature Reviews Rheumatology, 8*, 420-29. doi: 10.1038/nrrheum.2012.64

Uthaisangsook, S., Day, N.K., Bahna, S. L., Good, R. A., Haraguchi, S. (2002). Innate immunity and its role against infections. *Annals of Allergy, Asthma, and Immunology, 88*(3), 253-64. doi: 10.1016/S1081-1206(10)62005-4

Vladimer, G. I., Górna, M. W., & Superti-Furga, G. (2014). IFITs: Emerging Roles as Key Anti-Viral Proteins. *Frontiers in Immunology*, *5*, 94. doi:10.3389/fimmu.2014.00094

Weber, F., Haller, O., & Kochs, G. (1996). Nucleoprotein viral RNA and mRNA of Thogoto virus: a novel "cap-stealing" mechanism in tick-borne orthomyxoviruses?. *Journal of Virology*, *70*(12), 8361-7.

Weber, F., Haller, O., & Kochs, G. (2000). MxA GTPase blocks reporter gene expression of reconstituted Thogoto virus ribonucleoprotein complexes. *Journal of Virology*, *74*(1), 560-3. doi: 10.1128/JVI.74.1

Yang, Z., Liang, H., Zhou, Q., Li, Y., Chen, H., Ye, W., Chen, D., Fleming, J., Shu, H., & Liu, Y. (2012). Crystal structure of ISG54 reveals a novel RNA binding structure and potential functional mechanisms. *Cell Research*, *22*(9), 1328-38. doi: 10.1038/cr.2012.111